

Evidence for the band ferromagnetism in SrRuO_3 from neutron diffraction

S.N. Bushmeleva^{a,*}, V.Yu. Pomjakushin^{b,1}, E.V. Pomjakushina^{b,c,1},
D.V. Sheptyakov^b, A.M. Balagurov^a

^aFrank Laboratory of Neutron Physics, Joint Institute for Nuclear Research, Dubna, Moscow region 141980, Russian Federation

^bLaboratory for Neutron Scattering, ETH Zürich and Paul Scherrer Institute, CH-5232 Villigen PSI, Switzerland

^cLaboratory for Development and Methods, ETH Zürich and Paul Scherrer Institute, CH-5232 Villigen PSI, Switzerland

Received 26 October 2005; received in revised form 1 February 2006

Available online 6 March 2006

Abstract

The precise data on the crystal and magnetic structures of SrRuO_3 were obtained by neutron diffraction. The ferromagnetically ordered Ru moment amounts to $\mu_{\text{Ru}} = 1.63 \pm 0.06 \mu_B$ at $T = 10 \text{ K}$. This value agrees well with the results of recent electronic structure calculations, which predicted the possibility of band ferromagnetism in SrRuO_3 with the reduced ordered moment. The crystal structure of SrRuO_3 remains practically invariable in the temperature range of 1.5–290 K. We have also found that the “Invar effect” in SrRuO_3 (zero thermal expansion coefficient) is stipulated entirely by freezing of the mutual rotations/tilts of the oxygen octahedra below the phase transition into the ferromagnetic phase.

© 2006 Elsevier B.V. All rights reserved.

Keywords: Magnetic structure; Crystal structure; Neutron diffraction

1. Introduction

SrRuO_3 is the only known metallic ferromagnet ($T_c \approx 160$ –165 K) among the perovskite-related compounds with 4d element in the B-site of the unit cell. This fact and also its interesting transport properties, in particular the unusual behavior of electrical resistivity in the vicinity of T_c [1], are subject to a number of recent theoretical and experimental papers (see e.g. Ref. [2] and references therein). The magnetism in SrRuO_3 is caused by the Ru^{4+} cations which are in the $t_{2g}^4 e_g^0$ state (all 4d electrons at the t_{2g} level) with the spin $S = 1$ (low-spin state). Indeed, in some papers (see e.g. [3,4]) the paramagnetic moment, $\mu_{\text{eff}} = 2 \mu_B [S(S+1)]^{1/2}$, was found to be close to $2.8 \mu_B$, i.e. $S = 1$. The magnetization measurements on mono- and polycrystalline SrRuO_3 samples at low temperatures in magnetic fields up to 30 T [4] have yielded however, a

noticeably lower value of an ordered moment—less than $2 \mu_B$ (between 0.8 and $1.6 \mu_B$ in various papers), which could serve as an evidence of strong electron correlations in this compound. First principles calculations performed in Ref. [5], have shown the possibility of the band ferromagnetism in SrRuO_3 with reduced ordered moment, $\mu_{\text{Ru}} = 1.45 \mu_B$. Another approximation used in Refs. [6,7], also led to the FM state with $\mu_{\text{Ru}} = 1.17 \mu_B$ for the idealized cubic structure and with $\mu_{\text{Ru}} = 1.59 \mu_B$ for the real orthorhombic symmetry.

Several neutron diffraction experiments were performed with SrRuO_3 [2,8–12], but only the estimation of the ordered magnetic moment $\mu_{\text{Ru}} = 1.4 \pm 0.4 \mu_B$ was reported in Ref. [8]. The large experimental uncertainty was caused by the rapid dropdown of Ru^{4+} magnetic form-factor with increasing momentum transfer; a weak magnetic contribution was only detected in the first diffraction peak. In the other papers, the main attention was paid to the crystal structure of the compound at room and elevated temperatures (up to $\sim 1250 \text{ K}$ in Ref. [11]), where the orthorhombic symmetry of SrRuO_3 consecutively changes to tetragonal

*Corresponding author. Tel.: +70962162133; fax: +70962165484.

E-mail address: bushme@nf.jinr.ru (S.N. Bushmeleva).

¹On leave from FLNP, Joint Institute for Nuclear Research, Dubna.

($T_c = 825$ K) and then to cubic ($T_c = 945$ K) one [13]. Only in Ref. [10], the comparison of the SrRuO_3 crystal structures in the para- and the ferromagnetic (FM) phases (at $T = 290$ and 100 K, accordingly) was presented. No visible changes were found below the Curie temperature.

The detailed X-ray study of the temperature dependences of the unit-cell parameters of SrRuO_3 in the range of 12–300 K was carried out in Ref. [14]. It was shown that the onset of the ferromagnetic state is associated with an anomaly in the behavior of the lattice parameters and of the unit cell volume V_c : two of the three lattice constants are nearly temperature independent below $T_c \approx 160$ K (the “Invar effect”). From the comparison of the $V_c(T)$ dependence at $T \leq T_c$ with the Debye model and with the low-temperature magnetization behavior, and also with the $V_c(T)$ for CaRuO_3 , which is paramagnet, the authors [14] came to the conclusion about the interplay between the anomaly in the thermal expansion and the ferromagnetism in SrRuO_3 . The coupling between ferromagnetic ordering and the freeze of the oxygen octahedra tilts was confirmed recently in Ref. [15] after precise neutron diffraction refinement of the oxygen positions as a function of temperature.

Recently, we studied the $(\text{Nd}_{1-x}\text{Sr}_x)(\text{Mn}_{1-x}\text{Ru}_x)\text{O}_3$ compositions with x ranging from 0.125 to 0.875 [16], for which the consistent doping of the A- and the B-sublattices leads to the strong suppression of the double-exchange mechanism for Mn ions. It was shown in particular that for $x \geq 0.25$, the resulting ferromagnetic state is determined by the AFM coupling between Mn and Ru magnetic moments, and the FM coupling in the Mn–Mn and Ru–Ru pairs. The effective ordered magnetic moment of

this unusual long-range ferromagnetic state, which we called “statistical ferrimagnet” is linearly depended on the (Sr/Ru) content. The values of $\mu_{\text{Mn}} = 3.74 \pm 0.15 \mu_B$ and $\mu_{\text{Ru}} = 1.34 \pm 0.25 \mu_B$ were obtained by the linear approximation of the B-site moment as a function of x . The last value agrees well with the calculated ones [5–7], though $\sim 20\%$ uncertainty in μ_{Ru} did not allow making further quantitative conclusions.

In the present paper we report on the new experimental results for the low-temperature ordered magnetic moment in SrRuO_3 . The refined value of the low-temperature magnetic Ru moment ($\mu_{\text{Ru}} = 1.63 \pm 0.06 \mu_B$) agrees well with the calculated values [6,7]. Also, the behavior of the SrRuO_3 crystal structure was analyzed in the range from 1.5 to 290 K.

2. Experimental details

The SrRuO_3 powder sample was synthesized by the solid state reaction, from RuO_2 and SrCO_3 of the minimum purity of 99.99%. The respective amounts of starting reagents were mixed and calcinated at the temperatures 700–1150 °C during at least 100 h in air with several intermediate grindings.

Laboratory and synchrotron (Material Sciences Beamline, SLS synchrotron radiation facility at Paul Scherrer Institute, $\lambda = 0.9258 \text{ \AA}$) X-ray diffraction experiments (Fig. 1) showed the high degree of crystallinity, the absence of any impurities and the good correspondence of the refined crystal structure parameters to the known data. At room temperature, the structure of SrRuO_3 is typical for many perovskites: Pnma space group with

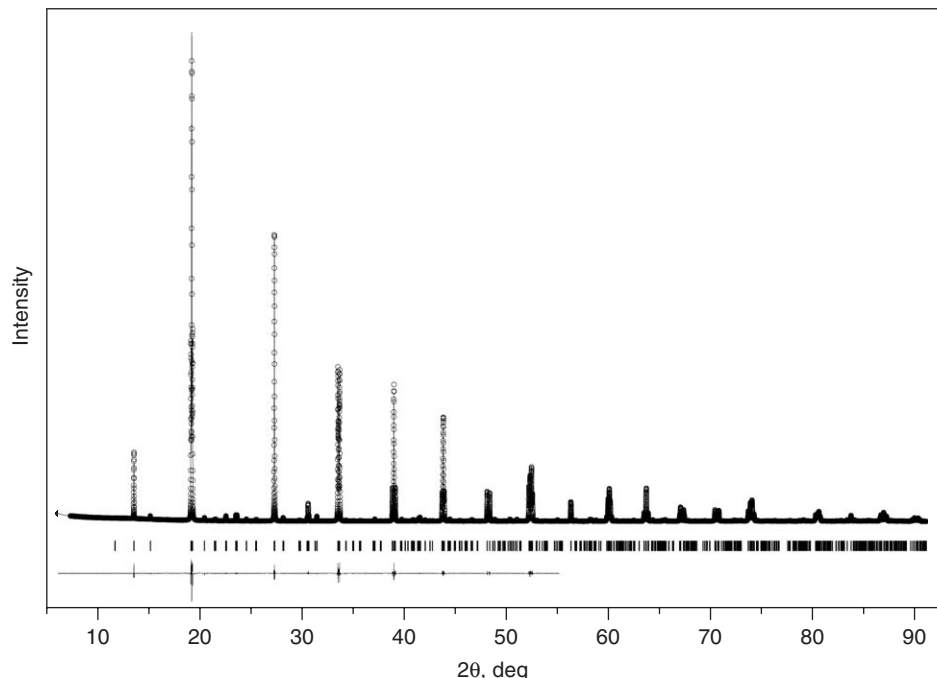


Fig. 1. Synchrotron X-ray diffraction pattern of SrRuO_3 measured at SLS/PSI at room temperature and processed by the Rietveld method. Synchrotron X-rays wavelength $\lambda = 0.92581 \text{ \AA}$. Difference curve is also shown. Ticks below the graph indicate the calculated peaks positions.

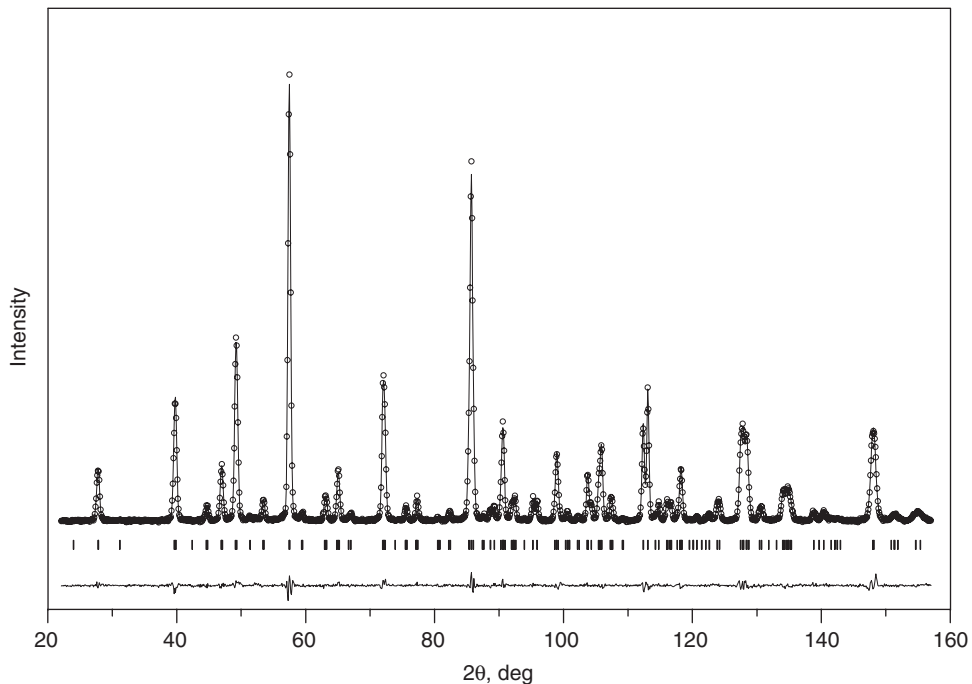


Fig. 2. Example of the Rietveld refinement pattern and difference plot of the neutron diffraction data (HRPT/SINQ) for SrRuO_3 at $T = 10\text{ K}$. The neutron wavelength $\lambda = 1.494\text{ \AA}$. The hkl -tics show calculated diffraction peaks positions.

$a \approx c \approx \sqrt{2}a_c \approx 5.55\text{ \AA}$, $b \approx 2a_c \approx 7.85\text{ \AA}$, where $a_c \approx 3.9\text{ \AA}$ is the lattice parameter of the ideal cubic perovskite.

Neutron powder diffraction experiments were carried out at SINQ spallation source of Paul Scherrer Institute. The crystal structure parameters in the temperature range of 1.5–290 K were refined from the data taken with the high-resolution diffractometer HRPT (the neutron wavelength $\lambda = 1.494\text{ \AA}$) [17]. The data on the magnetic structure were collected with the powder diffractometer DMC located on a supermirror-coated guide for cold neutrons at SINQ ($\lambda = 2.56\text{ \AA}$). The refinements of the crystal and the magnetic structure parameters were carried out with the FULLPROF program [18], with the use of its internal tables for the neutron scattering lengths. The magnetic structure refinement was performed with the magnetic form-factor of Ru^{1+} (there are no experimental data for Ru^{4+} form-factor in the literature). An example of the powder pattern obtained with HRPT and processed by Rietveld method is shown in Fig. 2.

3. Results and discussion

3.1. Crystal structure

The results of the structure refinement from the HRPT powder data at several temperatures are given in Table 1. The data at $T = 290\text{ K}$ are in the good agreement with the published neutron diffraction data [9–11]. The refined oxygen site occupancy (with the Sr- and Ru-site occupancies fixed to unity) is very close to the stoichiometric one

($n_O = 3.01 \pm 0.01$). The relative changes of the lattice parameters with temperature are shown in Fig. 3. All three parameters are decreasing below room temperature down to $T_c \approx 165\text{ K}$ with linear thermal expansion coefficient $\alpha \approx 8 \times 10^{-6}\text{ K}^{-1}$ (which is a typical value for oxides); at lower temperatures, α rapidly decreases and is close to zero below 100 K for a and b and below 60 K also for the c parameters. The interatomic distances $\text{Ru}-\text{O}1$, $\text{Ru}-\text{O}21$ and $\text{Ru}-\text{O}22$ (Fig. 4) are very close to each other in the whole temperature range. These data clearly show the absence of the Jahn–Teller distortions of the RuO_6 octahedra in correspondence with the hypothesis of the low-spin state of Ru^{4+} . The Jahn–Teller parameter

$\sigma_{JT} = \sqrt{1/3 \sum_i [(\text{Ru} - \text{O})_i - \langle \text{Ru} - \text{O} \rangle]^2}$ at room temperature is $\sim 2 \times 10^{-3}\text{ \AA}$, which is about 40 times smaller than that for LaMnO_3 , where Mn^{3+} is a Jahn–Teller active ion. Thus we conclude that the RuO_6 octahedra in SrRuO_3 are regular with $d_{\text{Ru}-\text{O}} = 1.986 \pm 0.002\text{ \AA}$ in the whole temperature range studied and the orthorhombically distorted SrRuO_3 structure is almost solely conditioned by the mutual rotations and tilts of oxygen octahedra. The two independent $\text{Ru}-\text{O}-\text{Ru}$ valence angles are close to 163° at room temperature and decrease by $\sim 1^\circ$ at the lowest temperatures (Fig. 5). In contrast to the $\text{Ru}-\text{O}$ distances the temperature dependences of $\text{Ru}-\text{O}-\text{Ru}$ angles indicate the phase transition into the FM state by the change of the slopes. The temperature position of this singularity corresponds to the sharp decrease (by a factor of ~ 30) of the linear thermal expansion coefficient for a and b unit-cell parameters. These data microscopically explain the Invar

Table 1
Structural parameters of SrRuO_3 at 1.5, 100 and 290 K, obtained by processing the data measured with HRPT diffractometer

Parameter/temperature	1.5 K	100 K	290 K
a (Å)	5.53168(3)	5.53052(5)	5.53533(5)
b (Å)	7.84543(4)	7.84449(8)	7.85105(9)
c (Å)	5.56648(2)	5.56593(4)	5.57286(5)
Sr (4c)			
x	0.02029(15)	0.0199(3)	0.0167(3)
y	0.25	0.25	0.25
z	0.9967(2)	0.9969(4)	0.9978(4)
B (Å ²)	0.12(1)	0.18(2)	0.54(3)
Ru (4b)			
x	0	0	0
y	0	0	0
z	0.5	0.5	0.5
B (Å ²)	0.005(11)	0.07(2)	0.14(2)
O1 (4c)			
x	0.4964(2)	0.4957(3)	0.4966(4)
y	0.25	0.25	0.25
z	0.0557(2)	0.0551	0.0522(5)
B (Å ²)	0.20(1)	0.24(2)	0.50(2)
O2 (8d)			
x	0.2784(1)	0.2791(2)	0.2771(2)
y	0.0281(1)	0.0279(2)	0.0268(2)
z	0.7221(1)	0.7219(2)	0.7237(3)
B (Å ²)	0.20(1)	0.24(2)	0.50(2)
Ru–O1 (Å)	1.986(1)	1.985(2)	1.984(2)
Ru–O21 (Å)	1.986(1)	1.984(1)	1.984(1)
Ru–O22 (Å)	1.987(1)	1.989(1)	1.988(2)
$\langle \text{Ru–O} \rangle$ (Å)	1.986	1.986	1.985
Ru–O1–Ru (deg.)	162.0(1)	162.2(2)	163.1(3)
Ru–O2–Ru (deg.)	161.9(3)	161.8(5)	162.8(5)

Space group Pnma (No. 62), the oxygen thermal parameters were constrained to be equal.

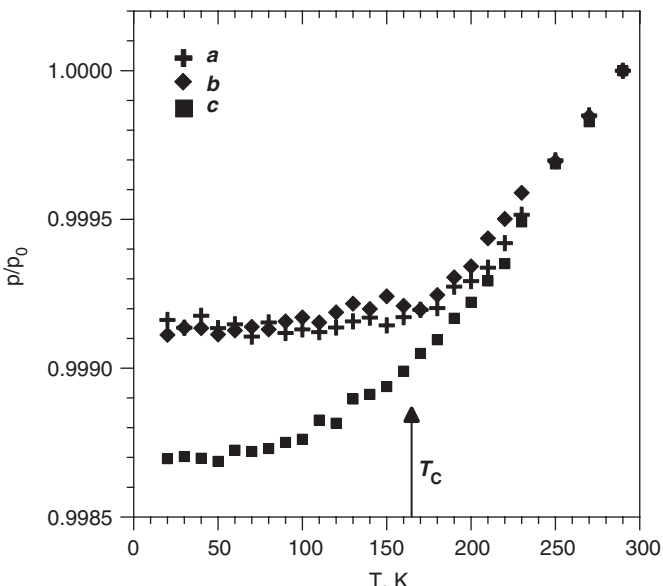


Fig. 3. Relative changes of the unit-cell parameters as functions of temperature, obtained from HRPT data. Arrow indicates the temperature of the FM transition. The errors are smaller than symbol sizes.

effect found for SrRuO_3 by Kiyama et al. [14]. The shortening of the lattice parameters is mainly due to the changes in mutual rotations and tilts of the oxygen octahedra. Correspondingly, the small value of α in the FM state is connected with the freezing of the RuO_6 octahedra rotations/tilts.

In general, the SrRuO_3 crystal structure undergoes only minor changes in the 1.5–290 K range. Taking into account the data from Ref. [13], one may conclude that its crystal structure is very stable even up to $T \approx 685$ K, at which temperature the transformation from Pnma into Imma space group occurs.

3.2. Magnetic structure

The neutron diffraction patterns collected at the low temperature with the DMC diffractometer show no additional lines, thus, excluding the possibility for the antiferromagnetic ordering at the level of $0.3 \mu_B$. This number is taken from our simulations, which show that for the particular case of SrRuO_3 , it is the threshold value of the antiferromagnetically ordered magnetic Ru moment accessible for the reliable determination from DMC powder diffraction data within a reasonable experimental time. Even if hypothetically overestimated, this value is not changing any of our conclusions drawn out below. The ferromagnetic state is revealed as a tiny increase in the intensities of some diffraction peaks (Fig. 6).

Because of the weak magnetic contribution to the diffraction intensities, the correlation between the value of Ru magnetic moment and its thermal motion is essential. To minimize that, the diffraction patterns measured at the DMC and the HRPT instruments were analyzed simultaneously: the high resolution and the wide range of d -spacings at HRPT ensured the precise refinement of the crystal structure parameters including the thermal factors, while the high intensity of cold neutrons at DMC effectively sorts out the magnetic contribution. From such a combined processing of the data from the two different diffractometers we obtained $\mu_{\text{Ru}} = 1.63 \pm 0.06 \mu_B$ at $T = 10$ K. The temperature dependence of the Ru magnetic moment is presented in Fig. 7. Its approximation by the empirical formula $\mu(T)/\mu(0) = [1 - (T/T_c)^q]^{\beta}$ leads to $T_c = 165 \pm 4$ K. The other free parameters in this relation are not well defined due to the small number of experimental points and large uncertainties.

The severe overlap of diffraction peaks does not allow determining unambiguously the direction of the magnetic moment in the cell. Though, the analysis of the line shapes of the (101)/(020) and the (220)/(022) peaks shows that the direction along a -axis is the most probable.

4. Conclusion

The results of the neutron-diffraction study of the SrRuO_3 crystal and magnetic structures in the wide temperature range are presented. The crystal structure of

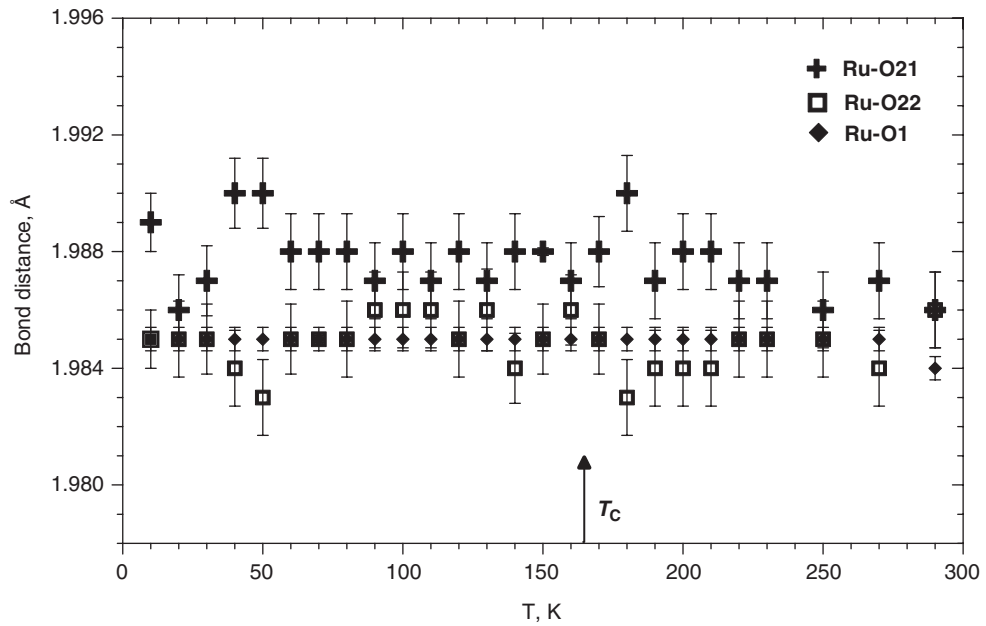


Fig. 4. Temperature dependences of the apical Ru–O1 and in-plane Ru–O21, Ru–O22 bond lengths. Arrow indicates the temperature of the FM transition. The solid lines are linear fit of the experimental points.

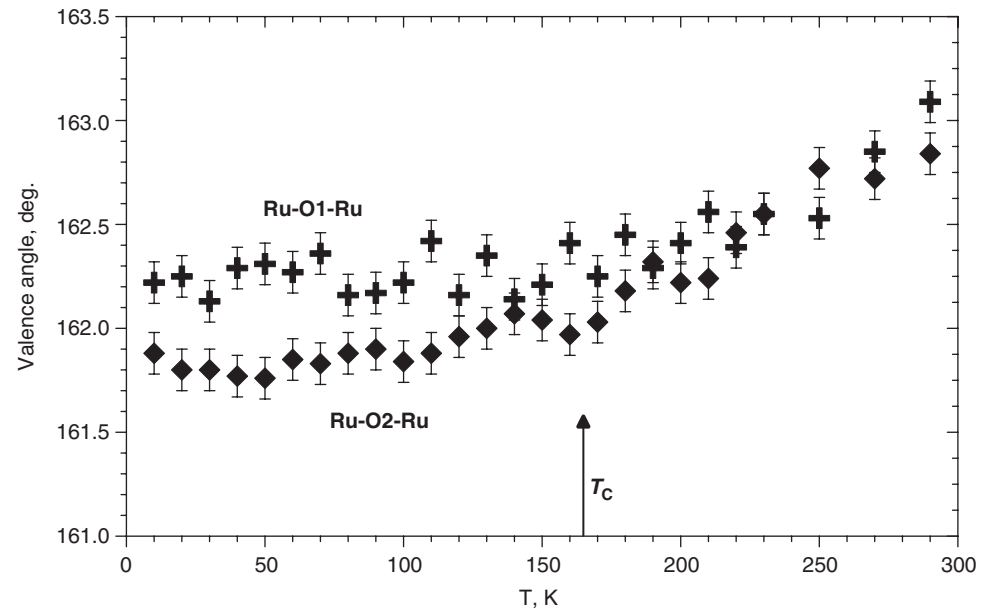


Fig. 5. Temperature dependences of the two independent valence angles. Arrow indicates the temperature of the transition into the FM state.

the compound is practically invariable in the temperature range 1.5–290 K. The temperature dependences of the lattice parameters of SrRuO_3 and correspondingly the Invar effect first found in Ref. [14] for the ferromagnetic state are conditioned by the mutual rotations and tilts of the oxygen octahedra, and not by the Ru–O bond lengths variations, which—within the accuracy of their determina-

tion—remain almost constant in the whole studied temperature range.

For the low-temperature ferromagnetically ordered state, the Ru magnetic moment is $\mu_{\text{Ru}} = 1.63 \pm 0.06 \mu_B$ at $T = 10 \text{ K}$. In the limits of experimental uncertainties it agrees well with $\mu_{\text{Ru}} = 1.59 \mu_B$ found from the electronic structure calculations carried out in Ref. [6].

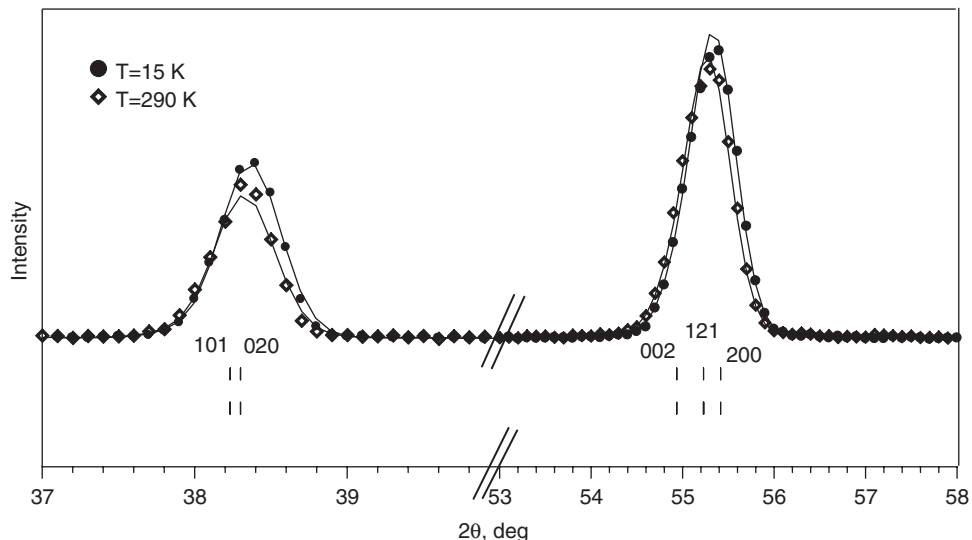


Fig. 6. Portions of the neutron diffraction patterns of SrRuO_3 measured with DMC at $T = 15$ and 290 K. A weak contribution of the FM intensity is seen.

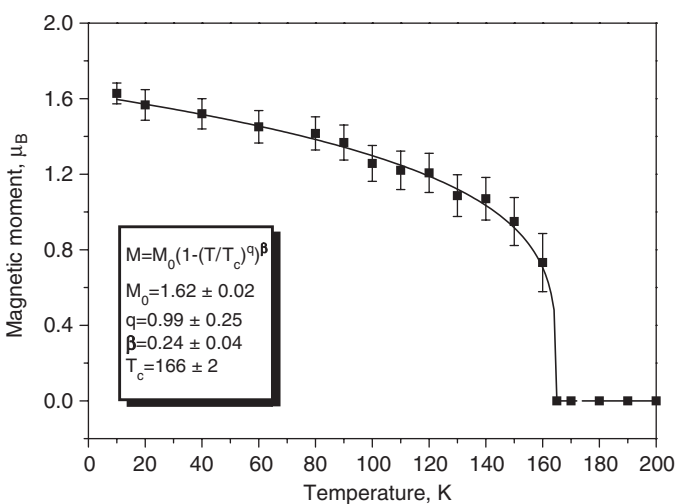


Fig. 7. Temperature dependence of the Ru average ordered magnetic moment. The experimental points were obtained from a combined refinement of the data measured with HRPT and DMC instruments. The calculated curve at $T \leq 160$ K corresponds to an empirical formula $\mu(T)/\mu(0) = [1 - (T/T_c)^q]^\beta$.

Our experimental data are thus in favor of the hypothesis of the band ferromagnetism in SrRuO_3 with the slightly reduced ordered moment.

Acknowledgements

The authors are grateful to N.A. Babushkina, A.R. Kaul and O.Yu. Gorbenko for the fruitful discussions which stimulated this work. The work was supported by the Russian Foundation for Basic Research (Project 03-02-16954). The neutron diffraction experiments were carried out with HRPT and DMC instruments at the Swiss Spallation Neutron Source SINQ, Paul Scherrer Institute,

Villigen, Switzerland. This work is also partially based on the experiments performed at the Swiss Light Source, Paul Scherrer Institute, Villigen, Switzerland.

References

- [1] L. Klein, J.S. Dodge, C.H. Ahn, G.J. Snyder, T.H. Geballe, M.R. Beasley, A. Kapitulnik, Phys. Rev. Lett. 77 (1996) 2774.
- [2] B. Dabrowski, O. Chmaissem, P.W. Klamut, S. Kolesnik, M. Maxwell, J. Mais, Y. Ito, B.D. Armstrong, J.D. Jorgensen, S. Short, Phys. Rev. B 70 (2004) 014423.
- [3] M. Itoh, M. Shikano, T. Shimura, Phys. Rev. B 51 (1995) 16432.
- [4] G. Cao, S. McCall, M. Shepard, J.E. Crow, R.P. Guertin, Phys. Rev. B 56 (1997) 321.
- [5] P.B. Allen, H. Berger, O. Chauvet, L. Forro, T. Jarlborg, A. Junod, B. Revaz, G. Santi, Phys. Rev. B 53 (1996) 4393.
- [6] D.J. Singh, J. Appl. Phys. 79 (1996) 4818.
- [7] I.I. Mazin, D.J. Singh, Phys. Rev. B 56 (1997) 2556.
- [8] J.M. Longo, P.M. Raccah, J.B. Goodenough, J. Appl. Phys. 39 (1968) 1327.
- [9] C.W. Jones, P.D. Battle, P. Lightfoot, W.T.A. Harrison, Acta Cryst. C 45 (1989) 365.
- [10] J.S. Gardner, G. Balakrishnan, D.McK. Paul, Physica C 252 (1995) 303.
- [11] B.C. Chakoumakos, S.E. Nagler, S.T. Misture, H.M. Christen, Physica B 241–243 (1998) 358.
- [12] B.J. Kennedy, B.A. Hunter, Phys. Rev. B 58 (1998) 653.
- [13] B.J. Kennedy, B.A. Hunter, J.R. Hester, Phys. Rev. B 65 (2002) 224103.
- [14] T. Kiyama, K. Yoshimura, K. Kosuge, Y. Ikeda, Y. Bando, Phys. Rev. B 54 (1996) R756.
- [15] B. Dabrowski, M. Avdeev, O. Chmaissem, S. Kolesnik, P.W. Klamut, M. Maxwell, J.D. Jorgensen, Phys. Rev. B 71 (2005) 104411.
- [16] A.M. Balagurov, S.N. Bushmeleva, V.Yu. Pomjakushin, D.V. Sheptyakov, V.A. Amelichev, O.Yu. Gorbenko, A.R. Kaul, E.A. Gan'shina, Phys. Rev. B 70 (2004) 014427.
- [17] P. Fischer, G. Frey, M. Koch, M. Könnecke, V. Pomjakushin, J. Schefer, R. Thut, N. Schlumpf, R. Bürge, U. Greuter, S. Bondt, E. Berruyer, Physica B 276 (2000) 146.
- [18] J. Rodríguez-Carvajal, Physica B 192 (1993) 55.